

## Recoil Properties of $\text{Sm}^{142}$ from Nuclear Reactions Induced by Heavy Ions. I. Samarium Compound Systems\*

MORTON KAPLAN AND RICHARD D. FINE†

*Department of Chemistry, Yale University, New Haven, Connecticut*

(Received 28 October 1963)

By means of thin-target differential-range experiments, we have measured the average ranges and range straggling of 72-min  $\text{Sm}^{142}$  recoils from a number of nuclear reactions induced by heavy ions. Beams of  $\text{Li}^6$ ,  $\text{Li}^7$ ,  $\text{B}^{10}$ ,  $\text{C}^{12}$ , and  $\text{N}^{14}$  with kinetic energies up to 10.5 MeV per nucleon were used in conjunction with targets of  $\text{Cs}^{133}$ ,  $\text{Ba}^{136}$ ,  $\text{Ba}^{137}$ ,  $\text{Ba}^{138}$ ,  $\text{La}^{139}$ , and  $\text{Pr}^{141}$ . A range-energy curve was obtained for  $\text{Sm}^{142}$  in Al, covering the region 2–10-MeV recoil energy. Strong evidence for a pure compound nucleus reaction mechanism is provided by (a) the uniqueness of the range-energy curve for all the reactions, (b) Gaussian-range distributions, and (c) direct comparison of the experimental ranges with stopping theory. The reaction  $\text{Nd}^{142}(\alpha, 4n)\text{Sm}^{142}$  was studied by integral range methods, and the average ranges in Nd were found to be consistent with theoretical expectations when projected ranges were corrected to true ranges. The experimental straggling parameters are compared with theoretical predictions of straggling inherent in the stopping process. For  $\text{Li}^6$  and  $\text{Li}^7$  experiments, where the recoil velocities are smaller than the Bohr velocity ( $2.2 \times 10^8$  cm/sec), an attempt is made to extract the range straggling due to the nuclear reaction. From this analysis, qualitative information is obtained about the average total energy removed by neutrons and photons.

### I. INTRODUCTION

WE have been studying the nature of heavy-ion-induced nuclear reactions by measuring the recoil properties of the heavy residual products. This technique<sup>1</sup> complements the information obtained by studying the light particles emitted from nuclear reactions, and has the virtue that specific reaction products may be isolated. Thus it is frequently possible to investigate a single nuclear reaction independently of all other processes which may be occurring simultaneously.

Our experiments yield the range distributions, in aluminum, of the specific nuclear-reaction product  $\text{Sm}^{142}$ . When a heavy ion collides with a target nucleus, all or some fraction of the incident linear momentum may be transferred in the interaction, and the highly excited system may then emit a number of particles, leaving behind a residual product nucleus. The linear momentum of this heavy recoil will be the vector sum of the momenta received from the bombarding heavy ion and that due to the emission of particles. The ranges that we measure are related to the projection of this vector sum on the incident-beam direction. If the fractional momentum transfer from the beam particle is high, then the average range of the reaction product will be determined primarily by the initial collision. The subsequent emission of particles will contribute to the distribution of ranges about the average value, but will affect the average itself only slightly.

Beams of  $\text{Li}^6$ ,  $\text{Li}^7$ ,  $\text{B}^{10}$ ,  $\text{C}^{12}$ , and  $\text{N}^{14}$  were used in conjunction with appropriate targets to yield samarium compound systems. By this we mean that the atomic

number of the target plus the atomic number of the beam particle was equal to 62 (Sm). Thus only neutrons may be emitted in the reactions if  $\text{Sm}^{142}$  is to be produced. We have chosen these relatively simple (HI,  $xn$ ) reactions for study, as it was felt that information obtained from them would be useful before attempting to understand more complex processes. In a succeeding paper we shall discuss the recoil behavior of  $\text{Sm}^{142}$  produced from Eu and Gd compound systems.

### II. EXPERIMENTAL

The nuclide  $\text{Sm}^{142}$  was chosen as a reaction product for study because its decay properties<sup>2</sup> permit convenient counting and identification.  $\text{Sm}^{142}$  decays with a half-life of 72-min to  $\text{Pm}^{142}$  which undergoes decay with a 34-sec half-life to stable  $\text{Nd}^{142}$ . Consequently, within a short time after an irradiation, any  $\text{Pm}^{142}$  produced directly will have decayed away, and the  $\text{Sm}^{142}$  will be in radioactive equilibrium with its daughter  $\text{Pm}^{142}$ . Both the parent and daughter decay by electron capture and positron emission. The maximum positron energies are<sup>2</sup> 1.03 MeV for  $\text{Sm}^{142}$  and 3.80 MeV for  $\text{Pm}^{142}$ , and by appropriate absorber arrangements it is possible to carry out radioactivity measurements which discriminate strongly in favor of  $\text{Pm}^{142}$ . The detected  $\text{Pm}^{142}$  is then a measure of the  $\text{Sm}^{142}$  produced in the nuclear reaction. For the work reported in this paper it is unnecessary to know any branching ratios in the decay chain, as only relative measurements are required.

Targets were prepared by vacuum evaporation of the desired material onto 0.00025-in. aluminum backings. La and Pr were evaporated as the metals, Cs as the nitrate, and Ba targets as the chlorides. Experiments with  $\text{Ba}^{136}$ ,  $\text{Ba}^{137}$ , and  $\text{Ba}^{138}$  were carried out with targets highly enriched in the desired isotope.<sup>3</sup> The

\* This work has been supported by the U. S. Atomic Energy Commission. Some of the results described in this paper were presented in preliminary form at the Third Conference on Reactions Between Complex Nuclei, held at Asilomar, Pacific Grove, California, April 1963.

† National Science Foundation Postdoctoral Fellow, 1962–63.

<sup>1</sup> B. G. Harvey, *Ann. Rev. Nucl. Sci.* **10**, 235 (1960).

<sup>2</sup> Thomas V. Marshall, University of California, Lawrence Radiation Laboratory Report UCRL-8740, 1960 (unpublished).

<sup>3</sup> Obtained from the Isotopes Department, Oak Ridge National Laboratory.

other targets are monoisotopic. The targets were always thin in comparison to the recoil range of the  $\text{Sm}^{142}$  product, and the actual thicknesses were determined by weighing the targets shortly after preparation. Uniformity of the target layers was estimated as better than a few percent by comparison of the thicknesses of different targets prepared in the same evaporation.

The recoil catcher foils were cut from commercial aluminum leaf 120–200  $\mu\text{g}/\text{cm}^2$  thick using a special punch of accurately known area. The foils were individually inspected for pinholes and nonuniformities by observing their appearance in front of a strong light. Only the better foils were selected for use (comprising about 15% of the total foils punched) and these foils were individually weighed to determine their thicknesses accurately.

A typical experiment consisted of assembling a target and a series of catcher foils in a water-cooled holder, and irradiating the stack with an appropriate heavy-ion beam from the Yale heavy ion linear accelerator (HILAC). The total catcher thickness was much greater than the extreme of the  $\text{Sm}^{142}$  recoil-range distribution, the extra foils serving as blanks to correct for activation in the aluminum catchers. After bombardment, the foils were separated and counted on a series of intercalibrated, end-window, gas-flow proportional counters. The samples were always counted through aluminum absorbers 432  $\text{mg}/\text{cm}^2$  thick, a procedure which effectively eliminated low-energy undesired radiations. (For example, beta groups of maximum energy 1.0, 1.5, and 2.0 MeV would be reduced in intensity by factors of about 1000, 25, and 10, respectively, in passing through the absorber. The efficiency of the detectors for counting gamma rays is only a few tenths of one percent.) The desired product,  $\text{Sm}^{142}$ , was detected by counting the high-energy positrons emitted in the decay of the  $\text{Pm}^{142}$  daughter.

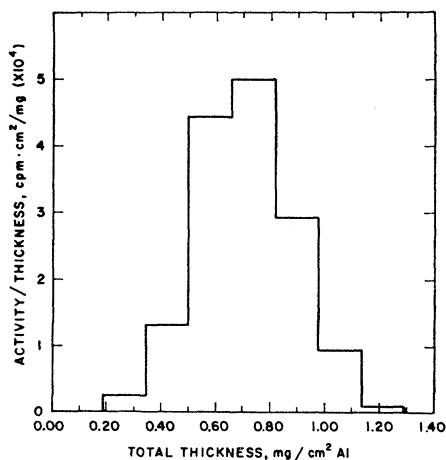


FIG. 1. Histogram of a typical differential-range experiment, showing the distribution of recoil  $\text{Sm}^{142}$  activity in the catcher foils. The data are for the reaction  $\text{Ba}^{138}(\text{C}^{12}, 8n)\text{Sm}^{142}$  at a bombarding energy of 121 MeV.

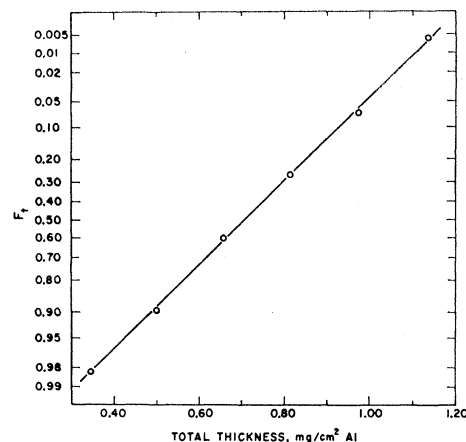


FIG. 2. Probability plot of the same data shown in Fig. 1.  $F_t$ , the fraction of the total recoil activity which passes through a catcher thickness  $t$ , is plotted on a probability scale against the total catcher thickness. In this representation, a straight line is indicative of a Gaussian distribution.

(This beta group of maximum energy 3.8 MeV is reduced in intensity by about a factor of 2 by the absorber.) Counting of the samples was carried out for a period of 4–5 h to permit the measurement of a decay curve for 72-min  $\text{Sm}^{142}$  over about 4 half-lives. After making the appropriate blank corrections for activation (due mostly to 32-min  $\text{Cl}^{34m}$  produced in the aluminum) the measured decay curves corresponded to pure  $\text{Sm}^{142}$  within an accuracy of about 2%. The blank corrections were typically of the order of 10–20%, but in experiments at bombarding energies where the  $\text{Sm}^{142}$  production cross section is small, the corrections corresponded to more than half of the total activity in catcher foils at the extremes of the range distributions. However, even in the less favorable cases, the accumulation of extensive decay curves tended to average out random errors in the blank subtractions, and the  $\text{Sm}^{142}$  present could be determined reliably.

The consistent observation of a 72-min half-life over more than an order of magnitude decay, in our various experiments with different target-beam combinations and a wide range of bombarding energies, supports our product-identification technique quite strongly. In addition, we have measured excitation functions for  $\text{Sm}^{142}$  production in these same reactions, using the same counting techniques, and find the shapes and peak positions of the excitation functions to be consistent with our interpretation.

### III. RESULTS

Figure 1 is a histogram of a typical differential-range experiment, showing the distribution of recoil  $\text{Sm}^{142}$  in the catcher foils. This particular case is for the reaction  $\text{Ba}^{138}(\text{C}^{12}, 8n)\text{Sm}^{142}$  at a bombarding energy of 121 MeV. We have plotted the measured activity in a catcher foil, divided by the foil thickness, as a function of the

TABLE I. Nuclear reactions leading to Sm<sup>142</sup>.

Pr <sup>141</sup> (Li <sup>6</sup> ,5n)	Ba <sup>137</sup> (C <sup>12</sup> ,7n)
Pr <sup>141</sup> (Li <sup>7</sup> ,6n)	Ba <sup>138</sup> (C <sup>12</sup> ,8n)
La <sup>139</sup> (B <sup>10</sup> ,7n)	Cs <sup>138</sup> (N <sup>14</sup> ,5n)
Ba <sup>136</sup> (C <sup>12</sup> ,6n)	

total thickness of (or penetration depth into) the foil stack. We have applied corrections for finite target thickness to all our differential-range data by adding one-half the target thickness (converted to aluminum equivalent) to the total catcher thickness. We can determine that the distribution of activity follows a Gaussian function by plotting on a probability scale the quantity  $F_t$ , defined as the fraction of the total activity which passes through a total catcher thickness  $t$ , against the total thickness.<sup>4</sup> On this type of plot, a Gaussian distribution will yield a straight line. Figure 2 shows such a probability plot for the same data as in Fig. 1. Thus we can represent the distribution of Sm<sup>142</sup> in the catcher foils by the equation

$$P(R)dR = \frac{1}{R_0\rho(2\pi)^{1/2}} \exp\left[-\left(\frac{R-R_0}{(2)^{1/2}R_0\rho}\right)^2\right]dR, \quad (1)$$

where  $R_0$  is the average range and  $\rho$  is the straggling parameter. The quantity  $\rho$  is a measure of the distribution in ranges about the average value. On the probability plot, as in Fig. 2, the catcher thickness at which  $F_t=0.5$  is the average range, and the slope of the line gives the straggling parameter.

Table I lists the different nuclear reactions which we have studied. For each reaction, measurements have been made at several bombarding energies. In every case the range distribution could be characterized by a Gaussian function, and the average ranges and straggling parameters were obtained from probability plots.

Table II summarizes our differential-range measurements. The first three columns list, respectively, the reacting system, the bombarding energy  $E_b$ , and the total available energy,  $(E_{c.m.}+Q)$ . Bombarding energies were computed from the range-energy curves of Northcliffe,<sup>5</sup> using the HILAC-beam full energy of 10.5 MeV/amu and the known thickness of aluminum used to degrade the beam to the desired energy. The total available energy was taken to be the sum of the energy in the center-of-mass system,  $E_{c.m.}$ , computed on the basis of full momentum transfer, and the  $Q$  value for the reaction. The various  $Q$  values were calculated using the atomic-mass tables of Everling, *et al.*<sup>6</sup> and the measured decay energetics of the mass-142 chain.<sup>2</sup>

Columns 4, 5, and 6 give, respectively, the target thickness, the average recoil range of Sm<sup>142</sup> in aluminum, and the straggling parameter. From the estimated uncertainties in thickness and radioactivity measurements, as well as the reproducibility of experiments, we believe our average range measurements to be accurate to about 5%. The straggling parameters are much more sensitive to experimental details, such as foil inhomogeneities and radioactivity measurements near the extremes of the range distributions, and consequently we feel that they are probably uncertain to about 20%.

We would like to use our range data to derive information about the nuclear-reaction mechanisms giving rise to the observed product. In order to do this, one needs to know the relationship between a measured

TABLE II. Results of differential-range experiments in aluminum for (HI, $xn$ ) reactions leading to Sm<sup>142</sup>.

Nuclear reaction	Bombarding energy, $E_b$ (MeV)	Total available energy, $(E_{c.m.}+Q)$ (MeV)	Target thickness, $W$ ( $\mu\text{g}/\text{cm}^2$ )	Average range, $R_0$ (mg/cm <sup>2</sup> )	Straggling parameter, $\rho$
Pr <sup>141</sup> +Li <sup>6</sup>	62.5	25.8	62	0.207	0.431
	62.5	25.8	61	0.205	0.455
	61.0	24.3	62	0.203	0.439
	58.3	21.7	67	0.198	0.411
	58.0	21.5	58	0.201	0.412
	55.4	19.0	61	0.184	0.431
	54.5	18.1	67	0.192	0.420
	53.5	17.1	58	0.173	0.421
	50.6	14.4	58	0.169	0.372
	49.1	12.9	58	0.171	0.405
46.3	10.2	58	0.149	0.498	
Pr <sup>141</sup> +Li <sup>7</sup>	71.8	26.9	64	0.279	0.386
	71.5	26.7	70	0.286	0.374
	68.9	24.1	68	0.269	0.394
	68.9	24.1	68	0.275	0.358
	65.8	21.2	76	0.267	0.378
	65.8	21.2	74	0.238	0.384
La <sup>139</sup> +B <sup>10</sup>	64.6	20.1	82	0.252	0.354
	103.7	42.9	124	0.513	0.275
	101.3	40.9	124	0.558	0.276
	95.3	35.2	115	0.489	0.272
	90.9	31.1	43	0.482	0.261
	87.4	27.8	49	0.470	0.238
	84.4	25.1	115	0.443	0.266
	81.2	22.1	105	0.421	0.217
76.7	17.9	123	0.423	0.274	
Ba <sup>136</sup> +C <sup>12</sup>	120.8	51.8	121	0.710	0.241
	109.8	41.7	115	0.652	0.219
	94.6	27.8	114	0.611	0.234
	80.3	14.6	114	0.500	0.253
Ba <sup>137</sup> +C <sup>12</sup>	113.0	37.8	116	0.672	0.252
	101.5	27.2	114	0.623	0.238
Ba <sup>138</sup> +C <sup>12</sup>	120.7	36.3	114	0.710	0.239
	118.8	34.5	125	0.700	0.238
	109.8	26.3	113	0.700	0.245
Cs <sup>138</sup> +N <sup>14</sup>	105.4	47.9	119	0.700	0.244
	100.7	43.4	147	0.718	0.238
	79.8	24.6	120	0.574	0.229
	71.8	17.4	141	0.548	0.256

<sup>4</sup> L. Winsberg and J. M. Alexander, Phys. Rev. **121**, 518 (1961).

<sup>5</sup> L. C. Northcliffe, Phys. Rev. **120**, 1744 (1960).

<sup>6</sup> F. Everling, L. A. König, J. H. E. Mattauch, and A. H. Wapstra, Nucl. Phys. **18**, 529 (1960).

range and the energy or velocity of the moving species. Experimental measurements of such relationships are rare for heavy atoms, and theoretical calculations are only now beginning to approach the problem satisfactorily (see Sec. IV). We have attempted to arrive at a range-energy curve for  $\text{Sm}^{142}$  by plotting our average ranges in aluminum against the energy the recoiling species would have if it were formed by a compound-nucleus reaction mechanism. With the assumptions of full momentum transfer from the beam projectile, and isotropic emission of particles in the center-of-mass system, the recoil energy is given by

$$E_R = A_b A_R E_b / (A_b + A_T)^2, \quad (2)$$

where the subscripts are  $b$  for bombarding particle,  $T$  for the target nucleus, and  $R$  for the recoil nucleus.  $A$  is the mass number and  $E$  is the kinetic energy. Figure 3 shows the results of this treatment. The measured average ranges, obtained from a number of different nuclear reactions over a wide range of energies, all lie on a single smooth curve. We interpret this as being a strong indication that we have calculated the recoil energies correctly, and that all the reactions we have studied proceed via a pure compound-nucleus mechanism. The solid curve in Fig. 3 is a theoretical range-energy curve derived from the recent detailed treatment of the stopping process by Lindhard, Scharff, and Schiøtt.<sup>7</sup> We will discuss this theory briefly in Sec. IV, but would like to point out here that the theoretical curve in Fig. 3 involves no normalization to our experimental data, and consequently the excellent agreement with our results provides independent evidence for the compound-nucleus nature of the nuclear reactions we are considering.

Alexander and Sisson<sup>8</sup> have made an extensive investigation of the recoil properties of  $\text{Tb}^{149}$  produced in a wide variety of heavy-ion induced reactions. From their data they have derived a range-energy curve for  $\text{Tb}^{149}$  in aluminum over the region 4–30 MeV. A comparison of their results with our data in Fig. 3 shows that the range-energy curves for  $\text{Tb}^{149}$  and  $\text{Sm}^{142}$  in aluminum are indistinguishable within the accuracy of the measurements ( $\sim 5\%$ ). From this one can infer that the recoil properties of heavy atoms do not change very rapidly with  $A$  and  $Z$  in this energy region.

We have also performed several experiments with the reaction  $\text{Nd}^{142}(\alpha, 4n)\text{Sm}^{142}$ . For this reaction, the recoil range of the product  $\text{Sm}^{142}$  in aluminum is too small to permit range-distribution measurements with our catcher foils. (The relatively small linear momentum of an alpha particle at energies where the reaction cross section is appreciable leads to the result that all the recoil activity is stopped in the first catcher foil.) Consequently we have carried out an integral type of

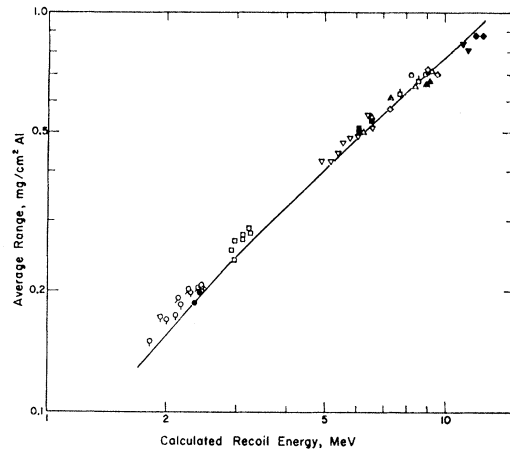


FIG. 3. Range-energy curve for  $\text{Sm}^{142}$  in aluminum. The open points are from experiments reported in this paper, and refer to the following systems: circles with tails,  $\text{Pr}^{141} + \text{Li}^6$ ; squares,  $\text{Pr}^{141} + \text{Li}^7$ ; inverted triangles,  $\text{La}^{139} + \text{B}^{10}$ ; triangles,  $\text{Ba}^{136} + \text{C}^{12}$ ; squares with tails,  $\text{Ba}^{137} + \text{C}^{12}$ ; circles,  $\text{Ba}^{138} + \text{C}^{12}$ ; diamonds,  $\text{Cs}^{133} + \text{N}^{14}$ . The filled points are for  $\text{Sm}^{142}$  produced from europium compound systems (taken from experiments described in the succeeding paper) as follows: circles,  $\text{Nd}^{142} + \text{Li}^6$ ; squares,  $\text{Ce}^{140} + \text{B}^{10}$ ; triangles,  $\text{La}^{139} + \text{C}^{12}$ ; inverted triangles,  $\text{Ba}^{136} + \text{N}^{14}$ ; diamonds,  $\text{Ba}^{137} + \text{N}^{14}$ . The solid line is a calculated range-energy curve based on the theory presented in Ref. 7.

experiment using Nd targets substantially thicker than the  $\text{Sm}^{142}$  recoil ranges. For these experiments, the average range in the target material (Nd) is given approximately by<sup>1</sup>

$$R_0 = FW, \quad (3)$$

where  $F$  is the fraction of the total activity which recoils out of the target and  $W$  is the target thickness.<sup>9</sup> Table III gives the results of these experiments, along with the average range values predicted by the theory of Lindhard, Scharff, and Schiøtt.<sup>7</sup> In making the theoretical computation, we have taken the recoil energy as given by Eq. (2) (i.e., we have assumed

TABLE III. Results of integral range experiments for the reaction  $\text{Nd}^{142}(\alpha, 4n)\text{Sm}^{142}$ .

Bombarding energy, $E_b$ (MeV)	Target thickness, $W$ (mg/cm <sup>2</sup> )	Fraction recoiling out, $F$	Average range, $R_0^a$ (mg/cm <sup>2</sup> Nd)	Average range (calc.) <sup>b</sup> (mg/cm <sup>2</sup> Nd)
47.4	0.339	0.470	0.159	0.219
45.8	0.320	0.456	0.146	0.210
45.8	0.324	0.491	0.159	0.210
44.2	0.315	0.437	0.138	0.202

<sup>a</sup> Average projected ranges along the beam direction; see Sec. IV.A.  
<sup>b</sup> Based on theory of Ref. 7.

<sup>9</sup> Equation (3) applies when the linear momentum imparted to the target by the beam is greater than the sum of all momenta due to the emission of particles. This results in a momentum component along the beam direction, and all recoils which leave the target go into the forward hemisphere. To check this point, an experiment was carried out with a target mounted backwards, the result being that an upper limit of 0.003 could be set for the fraction of the total activity emitted backwards.

<sup>7</sup> J. Lindhard, M. Scharff, and H. E. Schiøtt, Kgl. Danske Videnskab. Selskab, Mat. Fys. Medd. **33**, 14 (1963).

<sup>8</sup> J. M. Alexander and D. H. Sisson, Phys. Rev. **128**, 2288 (1962).

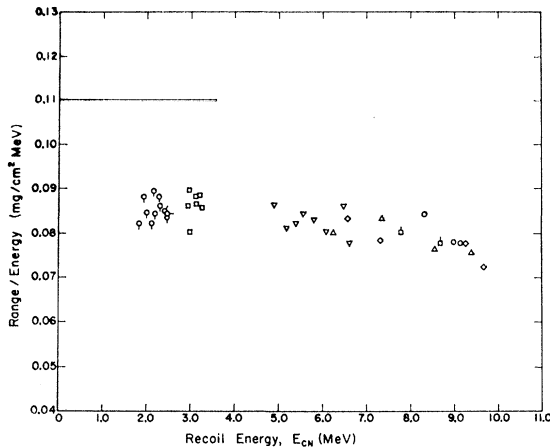


FIG. 4. Measured recoil ranges of  $\text{Sm}^{142}$  in aluminum divided by the recoil energies, and plotted against the recoil energy. The symbols are: circles with tails,  $\text{Pr}^{141}+\text{Li}^6$ ; squares,  $\text{Pr}^{141}+\text{Li}^7$ ; inverted triangles,  $\text{La}^{139}+\text{B}^{10}$ ; triangles,  $\text{Ba}^{136}+\text{C}^{12}$ ; squares with tails,  $\text{Ba}^{137}+\text{C}^{12}$ ; circles,  $\text{Ba}^{138}+\text{C}^{12}$ ; diamonds,  $\text{Cs}^{138}+\text{N}^{14}$ . The horizontal line is a theoretical prediction from Ref. 10 for  $v < v_0$ .

compound-nucleus formation). The experimental values are about 25% low in comparison with the calculated values. We have not investigated this discrepancy in detail, but will discuss a possible explanation in Sec. IV, below.

#### IV. DISCUSSION

##### A. Ranges

In the usual treatment of recoil experiments, it is customary to assume that the recoil distance  $R$  can be described by an equation of the form

$$R = k|v + V|^N, \quad (4)$$

where  $k$  and  $N$  are constants. The quantity  $v$  is the velocity of the center of mass, and  $V$  is the resultant velocity of the recoil atom in the center-of-mass system. Thus the resultant velocity in the laboratory system is the vector sum  $v + V$ . In the case of a compound nucleus reaction,  $v$  is the velocity of the compound nucleus, and  $V$  is the resultant additional velocity imparted to the recoil atom by the emission of particles. Calculation of the average range  $R_0$  requires a knowledge of the angular distribution of the vectors  $V$  with respect to  $v$ . Winsberg and Alexander<sup>4</sup> have shown that for  $v \gg V$  the average range  $R_0$  is given by a series expansion in  $V/v$ , with the leading term being

$$R_0 = kv^N. \quad (5)$$

The next term in the series enters as  $(V/v)^2$ , with a coefficient somewhat dependent on the form of the angular distribution. For the nuclear reactions we are considering here, we expect  $(V/v)^2$  to be small compared to unity, and consequently the average ranges should be given to a good approximation by Eq. (5). This

corresponds to saying that the average range is determined primarily by the momentum transfer in the collision between the bombarding heavy ion and the target nucleus and under these conditions it is appropriate to associate the measured average range  $R_0$  with the recoil energy given by Eq. (2).

Bohr's analysis<sup>10</sup> of the penetration of heavy charged particles through matter proposes the velocity of the electron in the hydrogen atom  $v_0$  as an approximate dividing line between stopping by electronic interactions ( $v > v_0$ ) and stopping by atomic collisions ( $v < v_0$ ). For velocities much greater than  $v_0$  ( $2.2 \times 10^8$  cm/sec), the average range should be proportional to the initial velocity, while for  $v < v_0$ , the average range should be proportional to the initial energy. For  $\text{Sm}^{142}$  recoils,  $v_0$  corresponds to 3.6-MeV recoil energy. From the data in Fig. 3, we find that the velocity exponent in Eq. (5) is given by  $N = 2.1$  over the energy range 2–3.5 MeV, and  $N = 1.7$  from 5–10 MeV. The  $\text{Tb}^{149}$  data of Alexander and Sisson<sup>8</sup> give  $N = 1.7$  from 5–10 MeV and  $N = 1.4$  from 15–30 MeV. Thus the observed ranges seem to follow the predicted velocity dependences rather well; i.e.,  $R_0$  is approximately proportional to energy for  $v < v_0$ , and tends towards proportionality to velocity for  $v > v_0$ .

The following expression has been derived<sup>10</sup> under the assumptions  $v < v_0$  and  $A_R \gg A_s$ ,

$$R_0 = BE, \quad (6)$$

where

$$B = 0.60 \frac{A_s(A_s + A_R) (Z_s^{2/3} + Z_R^{2/3})^{1/2}}{A_R Z_s Z_R}. \quad (7)$$

In these equations,  $Z$  and  $A$  are, respectively, the atomic and mass numbers with subscripts  $R$  for the recoiling atoms and  $s$  for the stopping atoms.  $R_0$  is in  $\text{mg}/\text{cm}^2$  and  $E$  is in MeV. We have compared our data for  $\text{Sm}^{142}$  with Eqs. (6) and (7) by plotting  $R_0/E$  against  $E$ , as shown in Fig. 4. In the energy region below 3.6 MeV, where Eqs. (6) and (7) would be expected to apply, our results do give a constant value for  $R_0/E$ . At energies corresponding to  $v > v_0$ , the points tend toward lower values. The solid line in Fig. 4 is the theoretical value of the ratio, as calculated from Eq. (7), and extends to  $v = v_0$ . Thus although our range results are indeed proportional to energy at low velocities, the constant of proportionality is about 25% lower than the theoretical prediction. Deviations of this type have been noted previously for  $\text{Tb}^{149}$  and  $\text{At}$  recoils.<sup>4</sup>

Recently, Lindhard, Scharff, and Schiøtt<sup>7</sup> (LSS) have carried out an extensive development of the theory of the range of heavy charged particles in matter. LSS are primarily concerned with ions of relatively low velocity, where stopping by atomic collisions (nuclear stopping) plays a significant role. Using a system of reduced (dimensionless) variables, LSS have computed a

<sup>10</sup> N. Bohr, Kgl. Danske Videnskab. Selskab, Mat. Fys. Medd. 18, No. 8 (1948).

universal nuclear-stopping cross-section curve, based on a Thomas-Fermi type potential. They have also given an expression for the electronic-stopping cross section taking this to be proportional to velocity. By integration of these functions and appropriate combination of the nuclear- and electronic-stopping contributions, LSS have derived a universal range-energy plot, in terms of their reduced variables. This plot consists of a family of curves, characterized by particular values of a parameter which depends in a complicated way on the masses and atomic numbers of the moving ion and the stopping medium. The static properties of the physical system enter through this parameter and through the definitions of the dimensionless range and energy variables. Thus the LSS treatment takes on its universal nature.

We have applied the LSS results to the stopping of  $\text{Sm}^{142}$  in aluminum, and have derived the range-energy curve shown in Fig. 3. The excellent agreement between theory and experiment is indeed gratifying, and points out the significant progress which has been made in the detailed understanding of the stopping process.

We would now like to discuss two approximations we have made in presenting our data above, and to estimate the effects arising from them. First, we mentioned that in writing Eq. (5) we were considering only the leading term in the series expansion of  $(V/v)$ . For an isotropic angular distribution of  $V$  in the center-of-mass system, Winsberg and Alexander<sup>4</sup> have derived

$$R_0 = kv^N [1 + \frac{1}{6}(N^2 + N - 2)(V/v)^2 + \dots]. \quad (8)$$

We shall estimate the magnitude of the term in  $(V/v)^2$  as follows.<sup>4</sup> If the distribution of ranges (range straggling) from the effects of the nuclear reaction is a Gaussian function with a (straggling) parameter  $\rho_n$ , then

$$\rho_n^2 = \langle (R - R_0)^2 \rangle / R_0^2 \quad (9)$$

which, for an isotropic angular distribution gives

$$\rho_n^2 = N^2 \langle V^2 \rangle / 3v^2. \quad (10)$$

As will be seen later in this section, we estimate from our  $\text{Li}^6$  and  $\text{Li}^7$  experiments (the largest effect)  $\rho_n^2 < \approx 0.1$ . Using Eq. (10) and  $N \cong 2$  from Fig. 3, we find the second term in Eq. (8) to be  $\approx 0.05$ . Thus, the ranges plotted in Fig. 3 should be reduced by a small amount to correspond to the recoil energies given by Eq. (2).

On the other hand, we have neglected any distinction between true ranges and projected ranges. What we actually measure is the projection of the true range onto the beam direction. For  $v \gg V$ , the emission of particles from the compound nucleus does not appreciably affect the direction of initial motion, but we must also consider scattering in the stopping medium. From this effect Lindhard and Scharff<sup>7,11</sup> find the ratio of true to projected

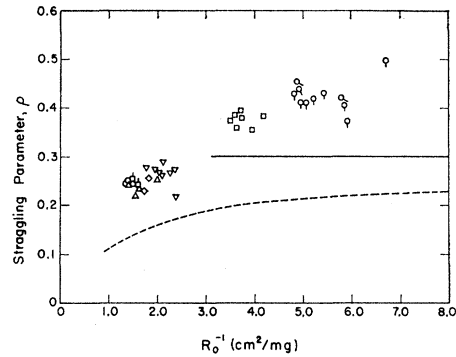


FIG. 5. Measured straggling parameters of  $\text{Sm}^{142}$  in aluminum plotted against the reciprocal of the average range. The symbols are: circles with tails,  $\text{Pr}^{141} + \text{Li}^6$ ; squares,  $\text{Pr}^{141} + \text{Li}^7$ ; inverted triangles,  $\text{La}^{139} + \text{B}^{10}$ ; triangles,  $\text{Ba}^{136} + \text{C}^{12}$ ; squares with tails,  $\text{Ba}^{137} + \text{C}^{12}$ ; circles,  $\text{Ba}^{138} + \text{C}^{12}$ ; diamonds,  $\text{Cs}^{138} + \text{N}^{14}$ . The solid line is a theoretical prediction from Eq. (12), for  $v < v_0$ , and represents only the straggling due to the stopping process. The dashed curve is derived from the theory in Ref. 7, and also represents only straggling due to stopping.

range to be approximately given by  $\{1 + \frac{1}{3}(A_s/A_R)\}$ . For  $\text{Sm}^{142}$  in aluminum, this amounts to a 6% correction, in the direction of making the observed ranges larger. Thus, the two small contributions we have omitted from our results in Fig. 3 will approximately cancel.

For our integral range experiments reported in Table III, the situation is somewhat different. Here, the mass of the moving ion is about the same as the mass of the stopping medium ( $\text{Sm}^{142}$  in Nd) and the correction from projected range to true range is about 30%. This will tend to bring the experimental values more nearly into agreement with the theoretical predictions. Because the thick-target experiments yield only the average ranges, and not the range distributions, we are unable to make any estimate of the effect of higher order terms (due to the nuclear reaction) which might modify Eq. (3).

## B. Range Straggling

Our differential-range experiments reported in Table II yield a straggling parameter  $\rho$ , which is a measure of the width of the Gaussian distribution represented by Eq. (1). The observed distribution in ranges arises from several contributions:  $\rho_s$ , the straggling inherent in the stopping process;  $\rho_n$ , the distribution of momenta due to particle emission in the nuclear reaction;  $\rho_w$ , the finite thickness of the target; and  $\rho_f$ , inhomogeneities in the catcher foils. These different effects combine approximately as the squares, to give the measured straggling parameter:

$$\rho^2 = \rho_s^2 + \rho_n^2 + \rho_w^2 + \rho_f^2. \quad (11)$$

We would like to be able to estimate  $\rho_n$  from our data, as this quantity contains information about the nuclear reaction. We show in Fig. 5 our measured values of  $\rho$  (listed in Table II) plotted as a function of the

<sup>11</sup> J. Lindhard and M. Scharff, Phys. Rev. 124, 128 (1961).

TABLE IV. Derived values of the nuclear reaction straggling parameter and the average total energy removed by neutrons ( $T_n$ ) and photons ( $T_\gamma$ ).

Reaction	$E_b$ (MeV)	$\rho^2$	$(\rho_n^2 + \rho_f^2)$	$T_n$ (MeV)	$T_\gamma$ (MeV)
Pr <sup>141</sup> +Li <sup>6</sup>	62.5	0.186	0.088	21.2	4.6
	62.5	0.207	0.109	26.2	-0.4 <sup>a</sup>
	61.0	0.193	0.095	22.4	1.9
	58.3	0.169	0.069	15.5	6.2
	58.0	0.170	0.073	16.3	5.2
	55.4	0.186	0.086	18.4	0.6
	54.5	0.176	0.075	15.8	2.3
	53.5	0.177	0.077	15.9	1.2
	50.6	0.138	0.037	7.2	7.2
	49.1	0.164	0.064	12.1	0.8
	46.3	0.248	0.144	25.7	-15.5 <sup>a</sup>
Pr <sup>141</sup> +Li <sup>7</sup>	71.8	0.149	0.054	17.3	9.6
	71.5	0.140	0.045	14.4	12.3
	68.9	0.155	0.059	18.2	5.9
	68.9	0.128	0.033	10.2	13.9
	65.8	0.143	0.046	13.5	7.7
	65.8	0.147	0.048	14.1	7.1
	64.6	0.125	0.025	7.2	12.9

<sup>a</sup> These negative energies are of no significance whatsoever, but simply result from large fluctuations in the experimental straggling-parameter data.

reciprocal of the average range. Probably the largest contribution to the observed straggling comes from the stopping process itself. For initial velocities much greater than  $v_0$ ,  $\rho_s$  should be inversely proportional to the range, whereas for velocities less than  $v_0$ ,  $\rho_s$  should be independent of energy.<sup>10,11</sup> Quantitative theoretical calculations of higher moments of the range are much more difficult to perform than range calculations themselves. For the low velocity region where  $\rho_s$  is independent of energy, Lindhard and Scharff<sup>11</sup> have derived the simple expression

$$\rho_s = \left[ \frac{2A_s A_R}{3(A_s + A_R)^2} \right]^{1/2}; \quad (v < \sim v_0, A_R \gg A_s). \quad (12)$$

The value of  $\rho_s$  for Sm<sup>142</sup> stopping in aluminum, as given by Eq. (12), is shown as the horizontal solid line in Fig. 5. We have terminated this line at the value of  $R_0^{-1}$  for which  $v = v_0$ . The dashed curve in Fig. 5 represents  $\rho_s$  as computed from the detailed treatment of Lindhard, Scharff, and Schiøtt.<sup>7</sup> In order to extract  $\rho_n$  from our experimental data, we must subtract out the straggling due to other sources, as indicated in Eq. (11). Our attempt to use the dashed curve in Fig. 5 as a measure of  $\rho_s$  has led to the result that  $(\rho_n^2 + \rho_f^2)$  is much larger than one would expect. Thus we find that either  $\rho_f^2$  is an important contributor to the observed straggling (i.e., the catcher foils are very nonuniform), or else the calculation gives values of  $\rho_s$  which are too small. We do not have any independent measure of the microscopic inhomogeneity of our catcher foils, but we consider it unlikely that this can account for all of the discrepancy.

We shall assume that at low velocities  $\rho_s$  is given approximately by Eq. (12). Our data for Li<sup>6</sup> and Li<sup>7</sup> bombardments of Pr<sup>141</sup> correspond to the energy region

where  $v < v_0$ , and the measured straggling parameters are substantially larger than the solid line in Fig. 5. We shall confine our analysis to these data, and subtract out the contribution due to the stopping process by means of Eq. (12). The effect of finite target thickness may be roughly estimated as  $\rho_w \cong 0.6W/2R_0$ , where  $W$  is the target thickness,  $R_0$  is the average range, and the factor 0.6 is the approximate relative stopping power of the target material and aluminum. As our targets were relatively thin,  $\rho_w$  does not make a very large contribution to the observed straggling, and this approximation should be satisfactory.

Having subtracted out the effects of  $\rho_s$  and  $\rho_w$ , by means of Eq. (11), we are left with values for the quantity  $(\rho_n^2 + \rho_f^2)$ . We list these derived values in Table IV, along with the observed straggling parameters, for our Li<sup>6</sup> and Li<sup>7</sup> experiments. As mentioned above, we have no quantitative estimate of  $\rho_f$ , and to proceed further we assume that  $\rho_f^2$  is small in comparison to  $\rho_n^2$ .

By considerations of detailed momentum balance, Simonoff and Alexander<sup>12</sup> have shown that if neutron emission from a compound nucleus is isotropic in the center-of-mass system, then the average total kinetic energy of the emitted neutrons  $T_n$  is related to  $\rho_n^2$  by

$$T_n = \frac{3\rho_n^2 E_b A_b (A_b + A_T + A_R)^2}{4N^2 (A_b + A_T)^2}. \quad (13)$$

In Eq. (13), the subscripts  $b$ ,  $T$ , and  $R$ , refer to the bombarding projectile, the target nucleus, and the recoil nucleus, respectively, and  $N$  is the exponent which appears in the range-velocity relation, Eq. (4). We have used the derived values of  $\rho_n^2$  (actually  $\rho_n^2 + \rho_f^2$ ) and our experimentally determined value of  $N$ , to compute the quantities  $T_n$  as given by Eq. (13). These are given in the 5th column of Table IV for each of our Li<sup>6</sup> and Li<sup>7</sup> experiments. The difference between the average total kinetic energies of emitted neutrons and the total available energies,  $(E_{c.m.} + Q)$ , given in Table II, presumably represents the average energy dissipated by photon emission. We list these latter values in the last column of Table IV as  $T_\gamma$ .

We wish to emphasize that the above analysis of our straggling-parameter data is rather crude. The experimental data show considerable scatter, and our understanding of straggling in the stopping process is still uncertain. Bearing these limitations in mind, we may qualitatively infer from the results in Table IV that most of the available energy is removed by the emitted neutrons, as expected. The apparently larger values of  $T_\gamma$  for Li<sup>7</sup> bombardments as compared to Li<sup>6</sup> experiments may be due to the use of a constant value of  $\rho_s$  [Eq. (12)] in our analysis, or may actually reflect the

<sup>12</sup> G. N. Simonoff and J. M. Alexander, University of California, Lawrence Radiation Laboratory Report UCRL-10099-Rev., 1962 (unpublished).

increasing importance of photon emission as more angular momentum is deposited in the reacting system.<sup>12,13</sup> It would be very informative to be able to determine the dependence of  $T_\gamma$  on total available energy and to extend the analysis to our data for other nuclear reactions. However, neither our straggling parameter measurements nor the theory are sufficiently accurate to permit such an attempt at the present time.

<sup>13</sup> J. R. Grover, *Phys. Rev.* **127**, 2142 (1962).

#### ACKNOWLEDGMENTS

We would like to thank Professor John M. Alexander for many stimulating discussions throughout the course of this work. The support of Professor E. Robert Beringer and the cooperation of the HILAC staff are gratefully appreciated. Our thanks are also due to Professor Richard Wolfgang and Dr. Ivor Preiss for making their experimental facilities available to us while our own equipment was being constructed.

## Recoil Properties of $\text{Sm}^{142}$ from Nuclear Reactions Induced by Heavy Ions. II. Europium and Gadolinium Compound Systems\*

MORTON KAPLAN

*Department of Chemistry, Yale University, New Haven, Connecticut*

(Received 28 October 1963)

Using thin-target recoil techniques, we have measured the average ranges and range straggling, in aluminum, of 72-min  $\text{Sm}^{142}$  produced in heavy-ion induced nuclear reactions. Eight different combinations of target and beam projectile were studied, five leading to Eu compound systems and three leading to Gd compound systems. In all cases the recoil-range distributions could be fitted by Gaussian functions. Comparison of the average ranges with a range-energy curve for  $\text{Sm}^{142}$  in Al provides evidence for a compound-nucleus mechanism in these reactions. The straggling parameters observed in reactions leading to Eu compound systems are in good agreement with those obtained for  $(\text{HI}, xn)$  reactions. In reactions leading to Gd compound systems, the straggling parameters are found to be anomalously large. It is suggested that these effects are due to alpha-particle emission from highly excited Gd compound nuclei, and an attempt is made to infer the kinematics associated with this process. The results of a relatively simple analysis of the straggling-parameter data show that the average kinetic energies of the emitted alpha particles are reasonable, but somewhat different for the several reactions investigated.

#### INTRODUCTION

IN the preceding paper<sup>1</sup> we have described the recoil properties of 72-min  $\text{Sm}^{142}$  produced from samarium compound systems. (By compound system we simply mean the sum of target atom and beam projectile.) In that work the observed  $\text{Sm}^{142}$  could only be formed by  $(\text{HI}, xn)$  reactions; i.e., only neutrons could be emitted. All the reactions studied were shown to occur by means of a pure compound-nucleus mechanism, and a range-energy curve was obtained for  $\text{Sm}^{142}$  in Al.

The present paper describes experiments in which the constraint on type of particle emitted has been relaxed. As the precursors of  $\text{Sm}^{142}$  in the radioactive decay chain are unknown, there is some ambiguity introduced into our knowledge of the nuclear reactions which are taking place. Thus, the observed product could arise either by  $(\text{HI}, xn)$  reactions followed by beta decay or by the emission of charged particles as well as neutrons in the reaction.

We have measured the average ranges and straggling

parameters, in aluminum, for  $\text{Sm}^{142}$  produced by the interaction of heavy ions with a number of targets. (For a discussion of the significance of these quantities, the reader is referred to the preceding paper<sup>1</sup> and the references given there.) Five different reactions leading to europium compound systems and three reactions leading to gadolinium compound systems have been investigated. The data obtained provide evidence that the observed  $\text{Sm}^{142}$  is formed by a compound-nucleus reaction mechanism, and an attempt is made to distinguish between competing reactions which would lead to the same product.

#### EXPERIMENTAL

The experimental procedure has been described in detail in the preceding paper,<sup>1</sup> and hence need only be summarized here. Stacks of thin targets and thin aluminum catcher foils, each of known area and individually weighed, were irradiated with an appropriate beam from the Yale heavy ion linear accelerator. For experiments with  $\text{Nd}^{142}$ ,  $\text{Ce}^{140}$ ,  $\text{Ba}^{136}$ , and  $\text{Ba}^{137}$ , the targets were highly enriched in the desired isotope.<sup>2</sup> The

\* This work has been supported by the U. S. Atomic Energy Commission.

<sup>1</sup> Morton Kaplan and Richard D. Fink, preceding paper, *Phys. Rev.* **134**, B30 (1964).

<sup>2</sup> Obtained from the Isotopes Department, Oak Ridge National Laboratory.